Structural Chemistry
https://doi.org/10.1007/s11224-021-01749-3

ORIGINAL RESEARCH

Another look at the structure of the $(H_2O)_n^{\bullet-}$ system: water anion vs. hydrated electron

Trinh Le Huyen[1,2] · Long Van Duong[3] · Devashis Majumdar[4] · Jerzy Leszczynski[4] · Minh Tho Nguyen[1,2]

Received: 3 February 2021 / Accepted: 8 February 2021

Abstract

Quantum chemical computations using both density functional theory and coupled-cluster theory methods, in conjunction with a polarizable continuum model for treatment of structures in solution, were carried out on a series of small water anions $[(H_2O)_n]^{\bullet-}$, n = 2, 3, 4, 5, and 16. Location of the excess electron was probed from a partition of electron densities using ELF and AIM techniques. For each size n of the $[(H_2O)_n]^{\bullet-}$ system, two distinct structural motifs are identified: a classical water radical anion formed by hydrogen bonds and a hydrated electron in which the excess electron is directly interacting with H atoms. Both motifs have comparable energy content and likely coexist in aqueous solution.

Keywords Hydrated electron · Water anion clusters · Water anions in solution

Introduction

A neutral molecule A can capture an electron leading to the formation of a bound radical anion $A^{\bullet-}$ with a usually small but positive adiabatic electron affinity. The excess electron can be either localized on an atom or a group of atoms or delocalized over the whole molecular skeleton [1]. When the energy level of its lowest unoccupied orbital (LUMO) is too high to accommodate the electron, the resulting radical anion $A^{\bullet-}$ could be higher in energy than the neutral A and thus not stabilized enough but remain in a metastable state in the gas phase. In a solution, the generated electron tends to spill into a cavity to capture solvent molecules forming a solvated entity. In fact, the electron continues to exist as a lone particle solvated by a cluster of A molecules, e $(A)_n$, in a continuum of A as the solvent. Solvated electron is a common phenomenon when the electron is radiolytically or photochemically generated in homogenous liquids, or at the interfaces of liquid and solids [2].

Hart and Boag [3] reported in 1962 the first experimental observation of hydrated electron produced upon radiolysis of water and characterized it by, among others, a broadband in the UV absorption spectrum centered at ~720 nm. Since then, its structural and spectroscopic properties, as well as its reactivities and dynamics, have extensively been investigated in a wealth of studies, experimental and theoretical alike. Previous results on the hydrated electron are extremely abundant and have critically been analyzed in book [4] and several review articles [5–14]. As it is not possible to mention here all relevant papers, we would refer to these review articles [5–14] including the most recent perspective article in 2019 [14] on the development of the subject.

In spite of such extensive studies, the geometrical and electronic structure of the hydrated electron remains a subject of a continuing debate. The original UV band centered at ~720 nm [3] and subsequent photoelectron [15, 17], vibrational [18, 19], and electronic [20–23] spectroscopic results pointed out a structure which is consistent with a "cavity model" [6, 24, 25] suggesting that the electron resides in a water solvent cavity with an average radius of ~2.4 Å, and is stabilized by hydrogen-bonded interactions between the electron and the positively charged H atoms of water molecules. Nevertheless, the questions as to when the electron goes

✉ Minh Tho Nguyen
nguyenminhtho@tdtu.edu.vn

1 Computational Chemistry Research Group, Ton Duc Thang University, Ho Chi Minh City, Vietnam

2 Faculty of Applied Sciences, Ton Duc Thang University, Ho Chi Minh City, Vietnam

3 Institute for Computational Science and Technology (ICST), Ho Chi Minh City, Vietnam

4 Interdisciplinary Center for Nanotoxicity, Department of Chemistry, Physics and Atmospheric Sciences, Jackson State University, Jackson, MS 39217, USA

Published online: 17 February 2021

within the cavity to form a solvated entity and why such phenomenon is occurring remain unanswered.

As a signature spectroscopic parameter, the optical spectrum of hydrated electron has theoretically been simulated using different approaches including the all-electron time-dependent density functional theory (TD-DFT) on small oligomers [26] and PCM-TD-DFT within a mixed quantum/classical framework (QM/MM) [27] and also molecular dynamics simulations [12].

A question of intense debate has been, and still is, concerning the actual number of water molecules involved in direct interaction with the electron to provide us with a good model for the hydrated electron. Earlier spectroscopic data revealed that for each size n, several isomeric forms of the e $(H_2O)_n$ complex are present in which the electron is connected with H atoms of distinct water molecules located in the liquid or frozen glass and hydrogen bonded to a network of other water molecules. Such a picture was widely accepted to represent the cavity model in which the long-range polarization potential of the solvent is an essential parameter. There has been discussion on a non-cavity model in which several water molecules are associated with the electron [28–31].

More recently, Herburger et al. [23] reported the electronic absorption spectra of water cluster anions $(H_2O)_n^{\bullet-}$ with $n \leq 200$ at $T = 80$ K and compared them with simulations from literature and experimental data for bulk hydrated electrons. These authors [23] pointed out that two almost isoenergetic electron binding motifs were seen for cluster sizes $20 \leq n \leq 40$, which were assigned to surface and partially embedded isomers. With increasing cluster size, while for $n \geq 50$ the partially embedded isomer prevails and the absorption is blue-shifted, in the size range from $n \approx 100$ the absorption spectrum is slightly red-shifted and similar to that of the bulk hydrated electron. Although the authors [23] argued that their results support the fact that the water anion clusters are reasonable model systems for hydrated electrons near the liquid−vacuum interface, a clear picture on the structure of the water anion clusters was not given.

The main experimental results supporting the predominance of an anionic water hexamer include the vertical electron detachment energy (VDE) which is associated with an unusually intense peak [16]. O–H stretching frequencies which show a frequency red shift are also a typical characteristic [9, 16, 18]. Some other studies pointed toward the importance of smaller-size hydrated electron [26, 32, 33]. Bartels and coworkers [26] carried out quantum chemical computations on small hydrated electron species embedded in a polarized continuum, and their computed results suggested that a *water tetramer* e $(H_2O)_4$ represents a dominant structural motif of the hydrated electron. Such a tetrahedral anion cluster whose electron occupies a central position interacting with *four* water H atoms, in fact, reproduce best the resonance Raman properties, radius of gyration, VDE, and hydration energy, as well as the EPR g-factor and hyperfine coupling constants [26, 34]. These constitute significant findings and can be served as starting models for further studies.

Regarding its chemical reactivity, the hydrated electron has been suggested to be involved in radiation chemistry, due to its formation upon radiolysis of water [35] and has been used as a reagent in charge-induced reactivity in different processes, due to its negatively charged nature [4]. Its most obvious process is its reaction with the surrounding water molecules whose kinetics have long been investigated [36]. A theoretical study using DFT-based molecular dynamics simulations [37] pointed out a complex mechanism of these reactions that involve not only proton transfers within the coordination sphere of the hydroxide anion but also diffusion of the H atom in its water solvent cavity.

Using quantum chemical computations, we recently demonstrated that the water anions, rather than hydrated electron model, involving four water molecules, can effectively be used to probe the mechanism and kinetics for the dissociation of water anions [38]. Some water anion isomers can dissociate when interacting with a water molecule, $[(H_2O)_n]^{\bullet-} + H_2O \rightarrow H^{\bullet}(H_2O)_m + OH^-(H_2O)_{n-m}$, through successive hydrogen transfers with moderate energy barriers. This process is basically a water-splitting in which H atom transfers take place within a water trimer, whereas other water molecules tend to stabilize transition structures through microsolvation rather than by direct participation. Calculated absolute rate constants for the reversed reaction $H^{\bullet}(H_2O)_2 + OH^-(H_2O)_2 \rightarrow [(H_2O)_4]^{\bullet-} + H_2O$ with both H and D isotopes, involving water oligomers, have been found to agree well with the experimentally evaluated kinetic results. On the other hand, the mechanism and kinetics of the reactions of the hydrated electron (e^-_{aq}) with the H_3O^+ and NH_4^+ cations were determined using quantum chemical computations with a polarized continuum model for treating structures in solution [39]. The NH_4^+ cation reacts with the hydrated electron, rather than with the water anions, involving a transition structure with H-tunneling, and the predicted rate constants agree well with available experimental results. These results lend on the one hand a kinetic support for the involvement of a water tetramer unit but suggest on the other hand that the identity of the reacting species could be different from each other depending on the reaction partners; the system could behave as either a hydrated electron or a water anion.

In view of the importance of the hydrated electron in different domains, and in particular with respect to the pending answers on the structure of the radical anion $[(H_2O)_n]^{\bullet-}$ system, we set out to have another look at their structures. For this purpose, we first redetermine, making use of quantum chemical computations, the geometrical and electronic structure of $[(H_2O)_n]^{\bullet-}$ system with $n = 2$, 3, 4, 5, and 16. Two different approaches to the electron localization in molecular systems, namely the ELF and AIM techniques, are subsequently used

with the aim to determine the whereabouts of the excess electron.

Computational details

All electronic structure theory calculations are conducted using the Gaussian 09 program package [40]. Geometry optimizations of the stationary points for both neutral and anionic systems are performed using the second-order perturbation theory (MP2) level for initial survey (Figure S1, SI file) and density functional theory (DFT) with the popular hybrid B3LYP functional in conjunction with the 6-311++G(3df,2p) basis set. The unrestricted formalism (UHF, UMP2, UB3LYP) is used for open-shell structures. For the treatment of systems in aqueous solution, based on previous studies [26, 41], the supermolecules considered are fully embedded in a continuum of water molecules using a polarizable continuum model (PCM) [42]. A recent computational study [41] on the $H^{\bullet}/H^{-}$ redox couple and the absolute hydration energy of H^{-} again showed that the PCM is quite suitable for the treatment of thermochemical properties of radicals and anions in aqueous solution.

The identity of each stationary point located is established by subsequent computations of harmonic vibrational frequencies at the same level. In order to improve the relative energies between isomers, single point total electronic energies of relevant equilibrium structures are calculated using (U)B3LYP-optimized geometries but with the coupled-cluster theory (U)CCSD(T) in conjunction with the correlation-consistent polarization aug-cc-pVTZ basis set, and also embedded in a water continuum using the PCM approach. In order to find the location of the excess electron, we use the electron localization function (ELF) technique [43] which partitions the total density into different basins. The atom-in-molecule (AIM) approach [44] is also used to probe the electron distribution.

Results and discussion

To simplify the presentation of calculated results, a large amount of data is given in Tables S1, S2 and Figures S1 and S2 of the SI file. Geometrical parameters determined using the second-order perturbation theory (MP2) level for the initial survey are given in Figure S1 (SI file).

Geometries of the radical anions $(H_2O)_n^{\bullet -}$: water anion vs. hydrated electron

Structures in the gas phase

Let us first consider again the small gas-phase water oligomers in two charge states that are served as references for further comparison. Figure 1 displays the shapes of optimized structures of both series of neutral and anionic water oligomers from the dimer to the pentamer, together with the main bond distances. As for a convention, each structure displayed in the following sections is denoted by **nx-gy** in which **n** = **1**, **2**, **3**, **4**, and **5** stand for the number of water molecules, **x** = **n, a** for neutral and anionic state, respectively, **g** for gas-phase structure, and **y** = **1**, **2…** for the isomers located with increasing relative energy. Unless otherwise noted, relative energies (ΔE) between isomers are obtained from (U)CCSD(T)/aug-cc-pvTZ + ZPE computations.

The structure **nx-g1** invariably corresponds to the most stable complex **nx-g**. Structures of the neutral water clusters have been the subject of an abundant number of previous studies, and thus deserve no further comments [45]. They are shown here only with the aim to focus on structural changes upon the addition of an excess electron. A few interesting points can be noted from Fig. 1:

i. Except for dimer **2a-g2**, all anionic oligomers become less compact. All O–H distances are in fact stretched upon electron addition, except for the intermolecular O–H distance in **2a-g2**, being 1.96 Å in **2n-g** and 1.94 Å in **2a-g2**. The increase of distance amounts up to 0.12 Å for intermolecular contacts.
ii. In the hydrogen-bonded dimer, while a *trans* configuration between the H atoms is well established for the neutral **2n-g1**, all geometry optimizations for the anion invariably converged to a *cis* configuration **2a-g2**. However, the novel anionic structure **2a-g1** whose neutral counterpart does not exist turns out to be more stable than the hydrogen-bonded **2a-g2** by 1.3 kcal/mol. The O–O and H–H distances in **2a-g1** are quite long, indicating the existence of interactions of four H atoms with the excess electron located at the center of the planar symmetrical species.
iii. The shape of the trimer is significantly changed upon electron addition. While anionic trimer tends to keep a cyclic framework, the nature of intermolecular contacts is changed from classical O–H–O hydrogen bond in neutral **3n-g1** to di-hydrogen H–H bond in anion **3a-g1** (Fig. 1). Such an arrangement appears to allow all H atoms to interact with the excess electron.

A water anion trimer structure having a chain geometry was previously reported to be the most stable form (from UCCSD(T) using UCCSD optimized geometry) [46]. The present **3a-g1** structure is calculated to be more stable than the structure in ref. [46] by only ~0.1 kcal/mol at the UCCSD(T)//B3LYP/6-311++(3df,2p) level. Accordingly, both structures can be regarded as isoenergetic and competitive for the ground state structure.

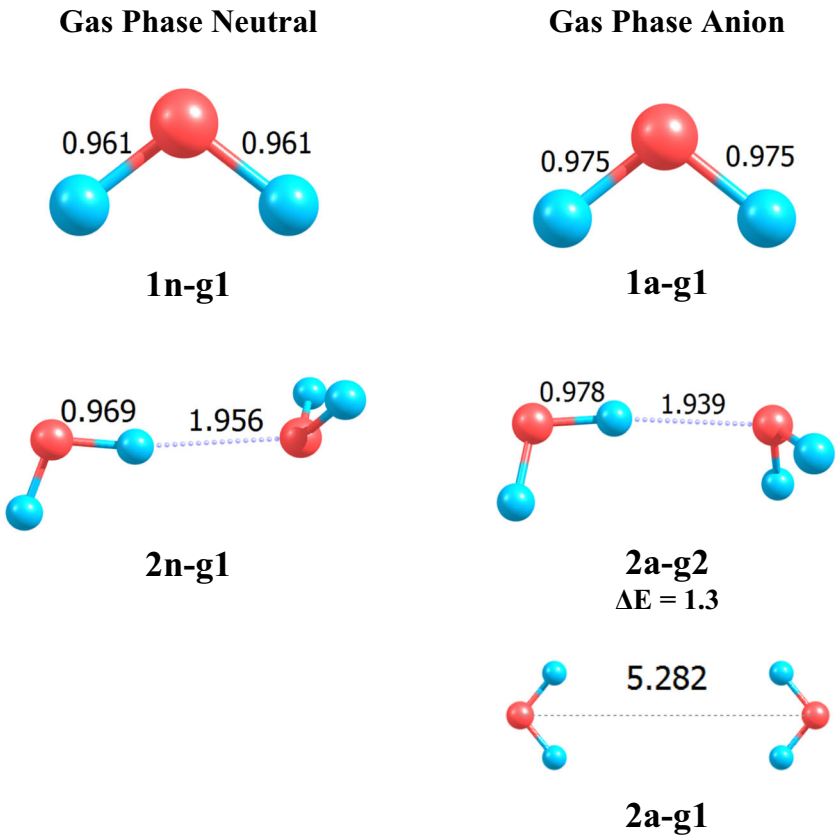

Fig. 1 Optimized geometric shapes and selected bond distances (Å) of small gas-phase neutral and anionic water oligomers, from monomer to pentamer ((U)B3LYP/6-311++G(3df,2p)). Relative energies (ΔE, kcal/mol) are obtained from (U)CCSD(T)/aug-cc-pVTZ + ZPE computations using (U)B3LYP geometries

iv. The tetrameric anion is also structurally changed in which the cyclic neutral shape of **4n-g1** is destroyed. While four oxygen atoms of **4n-g1** are located nearly in a plane, such a plane no longer exists in **4a-g1**. The shape of the stable anion **4a-g1** is apparently formed by interaction of dimer **2a-g1** with dimer **2a-g2**. Each water molecule of **2a-g1** interacts with one H atom of the H-acceptor monomer of **2a-g2** forming a classical O–H–O hydrogen bond, but with a longer O–H distance (1.99 Å).

Another way of considering **4a-g1** is as it is composed of a trimer plus a monomer. In the core trimer, both O–H–O and H–H contacts exist. The H–H distance of 3.01 Å (Fig. 1) is even shorter than that in **3a-g1**. Interaction of the fourth monomer with the trimer occurs via an O–H–O hydrogen bond.

v. Concerning the pentamer, the most stable five-membered cycle of neutral **5n-g1** disappears in going to anion **5a-g1**. The latter is apparently formed from interaction of dimer **2a-g2** with a distorted trimer in which a triangular H–H–H contact seems to emerge. Such an interaction gives rise to **5a-g1** which can also be viewed as arising from interaction of tetramer **4a-g1** with a fifth water monomer through H–O–H hydrogen bond.

vi. In the gas phase, water oligomers are characterized by small but negative electron affinities (EA), as the energy of each water anion is calculated to be higher than that of the corresponding neutral form by 10 to 20 kcal/mol (values at UCCSD(T)/aug-cc-pVTZ + ZPE). This is in line with previous efforts to compute the EA of water [45].

Structures in aqueous solution

Figure 2 displays optimized structures for both series of small neutral and negatively charged water oligomers when they are immersed in a continuum of aqueous solution. Their geometries are optimized using the (U)B3LYP/6-311+G(3df,2p) method in conjunction with a PCM approach for the treatment of water continuum. The validity of this approach has been discussed in previous studies [26, 38, 39, 41]. The main bond distances in each complex are also given in Fig. 2. For the neutral series, water oligomers tend keep their cyclic shape in going from gas-phase hydrogen-bonded complexes **nx-gy** (Fig. 1) to solvated **nx-sy** structures (**s** stands for structure in solution in this and following figures). Bond distances, in particular intermolecular distances, are only marginally

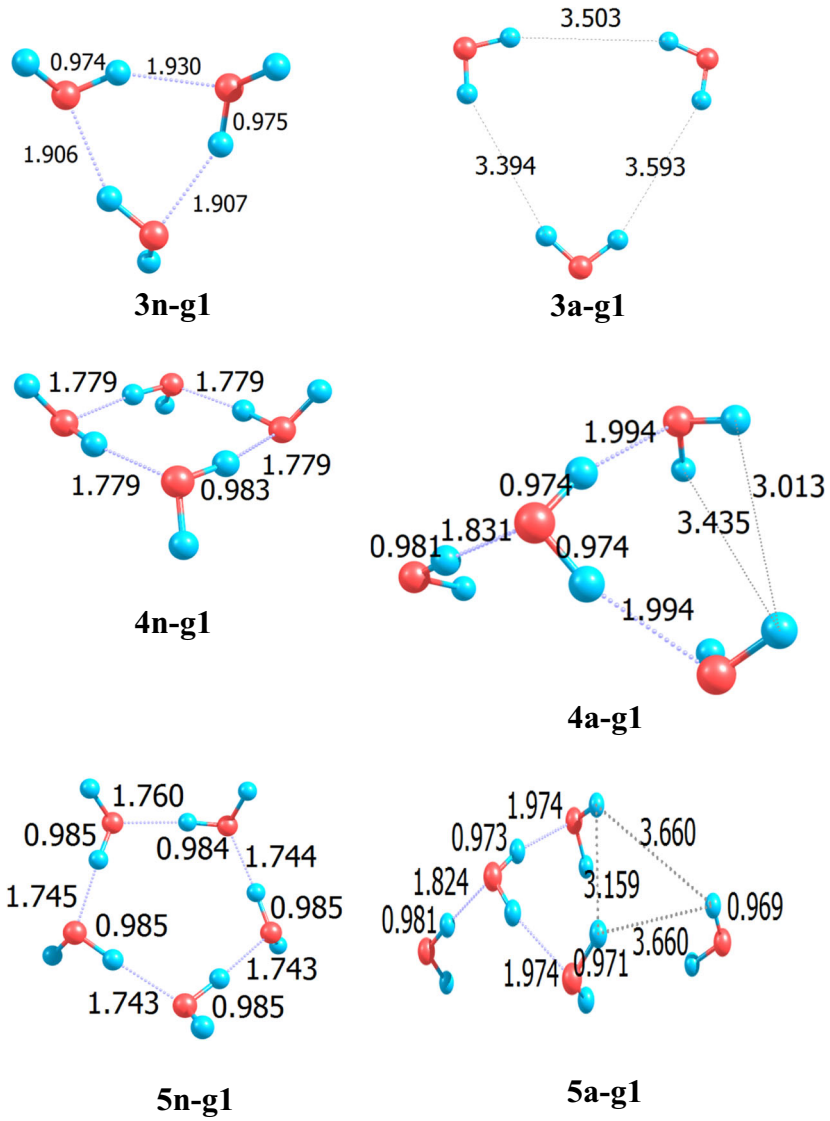

Fig. 1 continued.

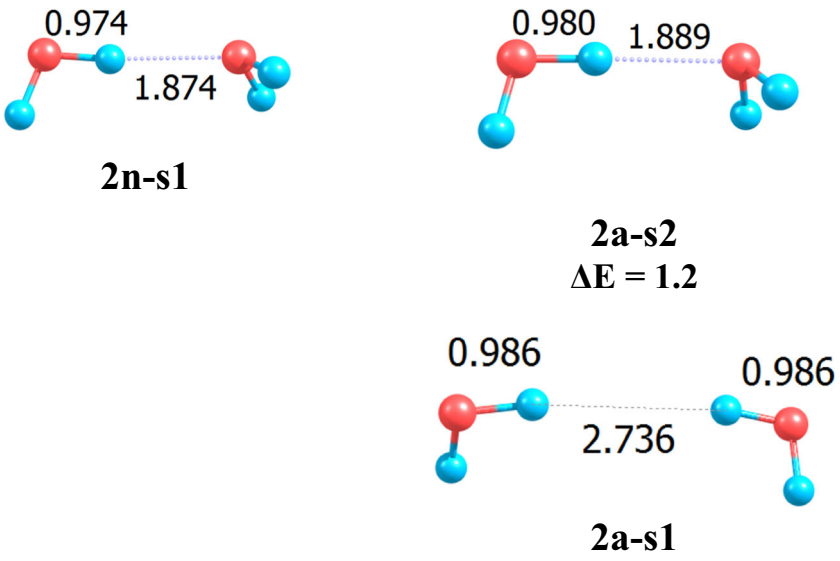

Fig. 2 Optimized geometric shapes and some bond distances (Å) of neutral and anionic dimers in aqueous solution (PCM-(U)B3LYP/6-311++G(3df,2p)). Relative energies (ΔE, in kcal/mol) are obtained from PCM-(U)CCSD(T)/aug-cc-pVTZ + ZPE computations based on B3LYP geometries

stretched upon solvation. A few remarkable structural features emerged from the results displayed in the following figures:

Dimers Both hydrogen-bonded dimers **2n-s1** and **2a-s2** exhibit now the same nuclear *cis* configuration, and intermolecular O…H distance in **2a-s** is again slightly stretched (Fig. 2). The most stable anion isomer turns out to be **2a-s1** which is ~1.2 kcal/mol more stable than **2a-s2**. This anion **2a-s1** can be characterized as the simplest hydrated electron in which the excess electron is located near the middle of both H atoms. The intermolecular H–H distance of 2.74 Å implies that the H-electron distance amounts to ~1.37 Å, which is expected to be a typical length for a H-electron bond.

The electronic structure of the dimer is further examined using the electron localization function (ELF) [43] which is a partition of the total electron density into different basins where electrons are concentrated. ELF maps often provide a complementary view to results obtained from other types of partition such as the AIM approach [44]. Figure 3 illustrates the ELF maps of both **2a-s1** and **2a-s2** structures.

The ELF map of **2a-s2** (Fig. 3a) points out that the excess electron in aqueous medium is found in basins located outside the water dimer entity, and in electrostatic interactions with non-bonded H atoms. As there are in the dimer three non-bonded H atoms and the excess electron is thus equally divided, each outside basin encloses about one-third of the electron (~0.33 electron). It can be viewed that a larger basin containing about two-thirds of electron appears around the two H atoms of the H-bond acceptor monomer.

The ELF map of **2a-s1** (Fig. 3b) clearly illustrates a direct interaction of two H-atoms with excess electron which is located around the middle of H–H contact. Such a distribution is further supported by the atom-in-molecule (AIM) map illustrated in Fig. 3c in which a bond critical point (BCP) is indeed identified at around the middle of both interacting H atom positions. There is a small charge transfer from the electron to each water molecule.

In summary, both geometric and electronic features demonstrate the existence of two distinct structural motifs, namely the hydrogen-bonded anion and the hydrated electron, for the dimeric $(H_2O)_2^{\bullet-}$. In view of their small relative energies (~2 kcal/mol), which lies within the expected error margin of ± 3 kcal/mol of the methods employed (with incomplete basis set and continuum model), both structures can be regarded as having a nearly degenerate energy content.

Trimers In the neutral state, both cyclic **3n-s1** and open **3n-s2** forms are found with a very small energy difference (Fig. 4). For anion trimer, lower-lying structures found include **3a-s1**

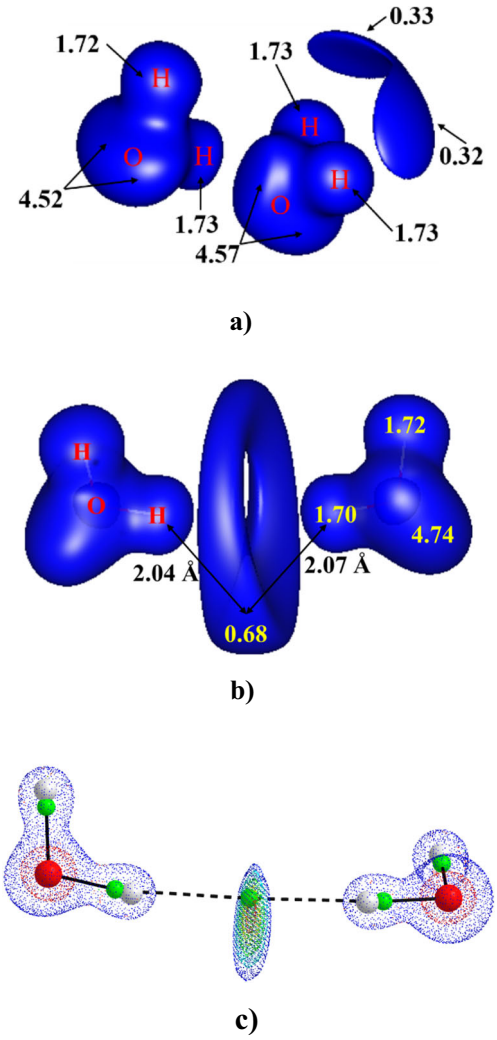

Fig. 3 ELF maps of the species in aqueous solution **a 2a-s2** and **b 2a-s1** and **c** AIM map of **2a-s1**. Values indicate amounts of electron concentrated in basins (UB3LY/6-311++G(3df,2p))

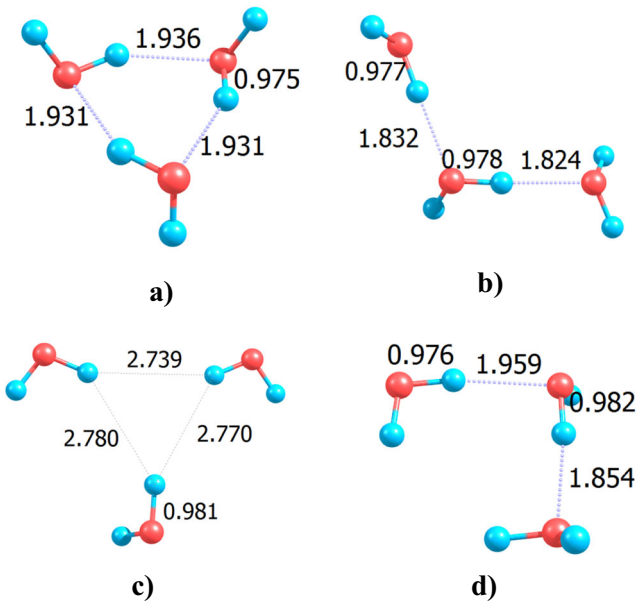

Fig. 4 Optimized geometries and some bond distances (Å) in aqueous solution of neutral trimer **a 3n-s1** and **b 3n-s2** and anionic trimer **c 3a-s1** and **d 3a-s2** (PCM-(U)B3LYP/6-311++G(3df,2p))

and **3a-s2** (Fig. 4). The optimized shape of **3a-s1** is in good agreement with a recent theoretical study [15]. This hydrated form is basically formed upon attachment of the third water molecule to the dimeric **2a-s1** via an electron-H contact and is calculated to be ~2 kcal/mol below **3a-s2**. The latter is also formed upon interaction of the third water molecule to the dimer **2a-s2** by an additional O–H–O hydrogen bond and can be regarded as a water trimer anion. No O–O–O cyclic anion similar to the neutral **3n-s1** can be found. Geometry optimizations for anion starting from neutral **3n-s1** and **3n-s2** geometries invariably lead to anion **3a-s2** which is ~2 kcal/mol higher than **3a-s1**. There are some other isomers such as those in which one monomer uses both H-atoms to interact with O-atoms to two other monomers. These isomers are however > 2 kcal/mol higher in energy than **3a-s1**.

As in the dimeric case, the shape of the more stable trimer anion **3a-s1** basically differs from that of neutral trimer **3n-s1** (Fig. 4) or gas phase trimer anion **3a-g1** (Fig. 1). A new and interesting feature of **3a-s1** is that a triangle is formed from three H atoms, each from one water molecule, and all of them appear to be interacting with the excess electron located at the triangular center. The H…H distance of ~2.7 Å of **3a-s1** triangle is rather large, but this points out that while H–H repulsion is not effective, attractive, and stabilizing electron-H atom interactions end up favoring the hydrated structure **3a-s1**. The electron-H distance amounts now to ~1.95 Å.

Figure 5 shows the ELF map of trimer **3a-s1**. Each water monomer bears ~8.1 valence electrons. About one-third of the excess electron is transferred to monomers, and a large part is localized in the basins situated at the center of a H–H–H triangle (> 0.6 electron). Overall, both geometric and electronic aspects again confirm that trimeric anion **3a-s1** behaves

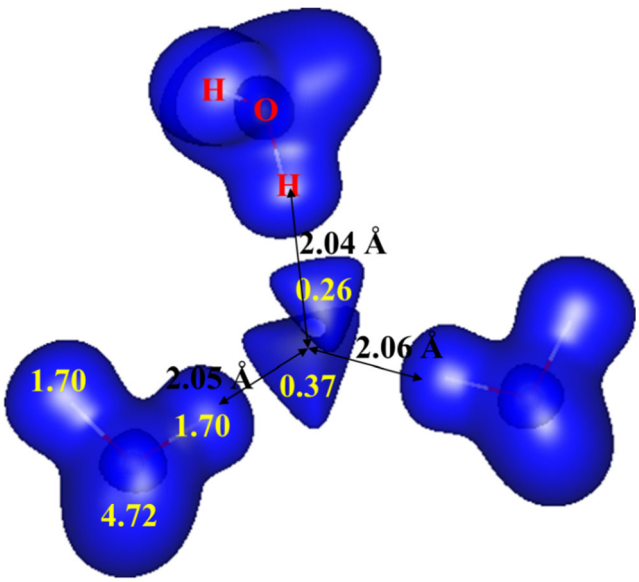

Fig. 5 The ELF map of trimeric hydrated electron in aqueous solution **3a-s1**. Values indicate amounts of electron concentrated in basins (UB3LYP/6-311++G(3df,2p))

effectively as a hydrated electron e $(H_2O)_3$ whose central electron is surrounded by three water molecules via attractive electron-H interactions.

Tetramers The geometry of the neutral tetramer in solution **4n-s1** (Fig. 6a) is basically similar to that of its gas phase counterpart **4n-g1** (Fig. 1) and is characterized by a four-membered cycle made by four oxygen atoms. In contrast, the geometry of tetrameric anion turns out to drastically be changed following solvation. Geometry optimizations for the anion starting from any point close to neutral **4n-s1** leads to two different lower-energy minima **4a-s1** and **4a-s2** (Fig. 6b, c). While **4a-s2** has a shape similar to that of conventional neutral **4n-s1**, the equally stable anionic isomer **4a-s1** has a tetrahedral form. For the sake of visualizing, Figure S2 (SI file) shows different perspective views of this structure.

An energy difference of ~3 kcal/mol is found in favor of the novel tetramer **4a-s1** with respect to the classical **4 s-s2**, which was also reported in a previous study [47]. This finding also confirms the results reported in a previous theoretical study [26]. **4a-s1** corresponds to a tetrahedron made by four H atoms, each coming from one monomer. The four H atoms are apparently directed toward the excess electron situated at the center of the tetrahedron. Stabilizing electrostatic electron-H atom interactions again favor the emergence of tetrahedral anionic tetramer **4a-s1**. As in the case of trimers, there are some other isomers such as those in which one monomer uses both H-atoms to interact with O-atoms to two other monomers. These isomers turn out to be higher in energy than **4a-s1**, and they are not further considered.

Figure 7 displays both the ELF and AIM critical point maps of **4a-s1**. Basins of electrons illustrated in Fig. 7a are found using the value ELF = 0.8. These basins disappear when a value ELF < 0.8 is used, which means that they are localized basins. Again, each water monomer contains ~8.1 valence electrons, as charge transfer from the electron is significant (one half of electron). The central basins enclose about one-half of electron. Such a picture of electron distribution is further supported by AIM critical points displayed in Fig. 7b. A type of cage critical point clearly emerges at the center of the 4H-tetrahedron **4a-s1**. While **4a-s1** again behaves as a hydrated electron, **4a-s2** looks like a more conventional water anion.

Pentamers The neutral **5n-s1** displayed in Fig. 8 exhibits a shape similar to its gas phase counterpart **5n-g1** (Fig. 1). Two different stable structures having a similar energy content are located for the pentameric anion, and both significantly differ from the neutral pentamer (Fig. 8). Accordingly, the shape of both anions **5a-s1** and **5a-s2** can be regarded as a complex formed from a stable tetramer **4a-s1** or **4a-s2** through interaction with one monomer. The fifth monomer is expected to be placed at different positions around a tetramer leading to a variety of complexes having comparable energy content.

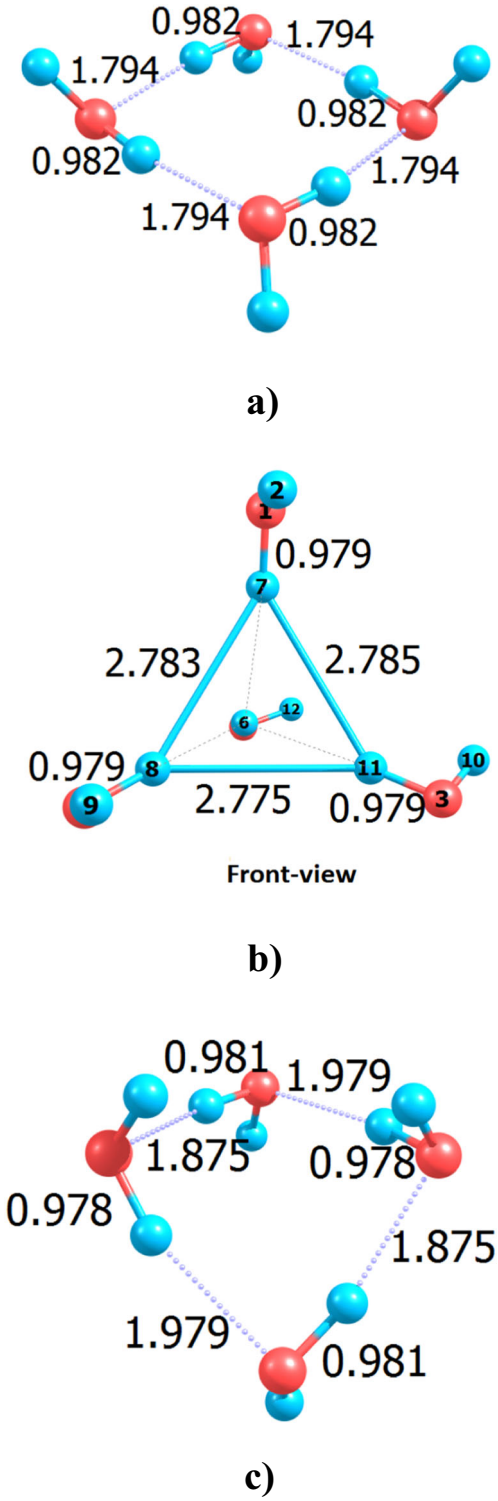

Fig. 6 Optimized geometric shapes and some bond distances (Å) in aqueous solution of **a** neutral **4n-s1**, **b** anionic **4a-s1**, and c anionic **4a-s2** (PCM-B3LYP/6-311++G(3df,2p)). Relative energies (ΔE, in kcal/mol) are obtained from PCM-(U)CCSD(T)/aug-cc-pVTZ + ZPE computations

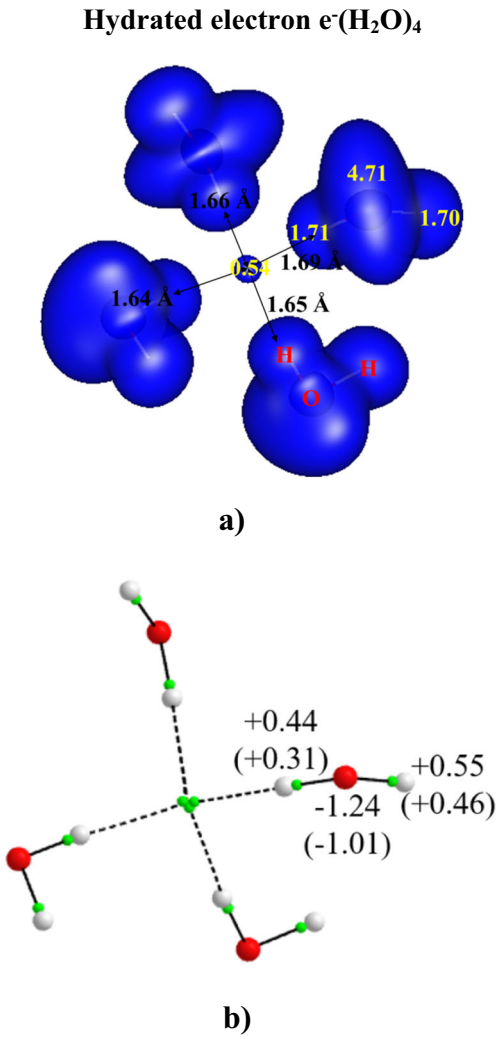

Fig. 7 Electron distribution of hydrated electron $e^-(H_2O)_4$ in aqueous solution **4a-s1**: **a** ELF map at ELF = 0.8. Values indicate the amounts of electrons concentrated in basins, and **b** atom-in-molecule critical points. Values are AIM net charges. NBO charges are given in parentheses (UB3LYP/6-311++G(3df,2p))

The hydrated electron **5a-s2** (formed from **4a-s1**) is computed to be at only 1.1 kcal/mol less stable than pentamer anion **5a-s1** (formed from **4a-s2** with some distortions). Again, within the expected accuracy of the methods employed, either the UCCSD(T) or the UB3LYP, being ± 3 kcal/mol on relative energies, both isomers are energetically quasi-degenerate and competing for the corresponding ground state. As for a further calibration, **5a-s1** remains the more stable structure when using different density functionals such as the UwB97XD, UwB97X, and UM06-2X with the same 6-311++G(3df,2p) basis set for geometry optimizations.

Larger oligomers Larger oligomers are successively explored for the anions. A consistent pattern appears to emerge in the formation of larger size anions. As in the case of pentamer, tetramer **4a-s1** (Fig. 6) appears to play the role of a building block from which additional water molecules are attached through classical hydrogen bonds whose configurations are

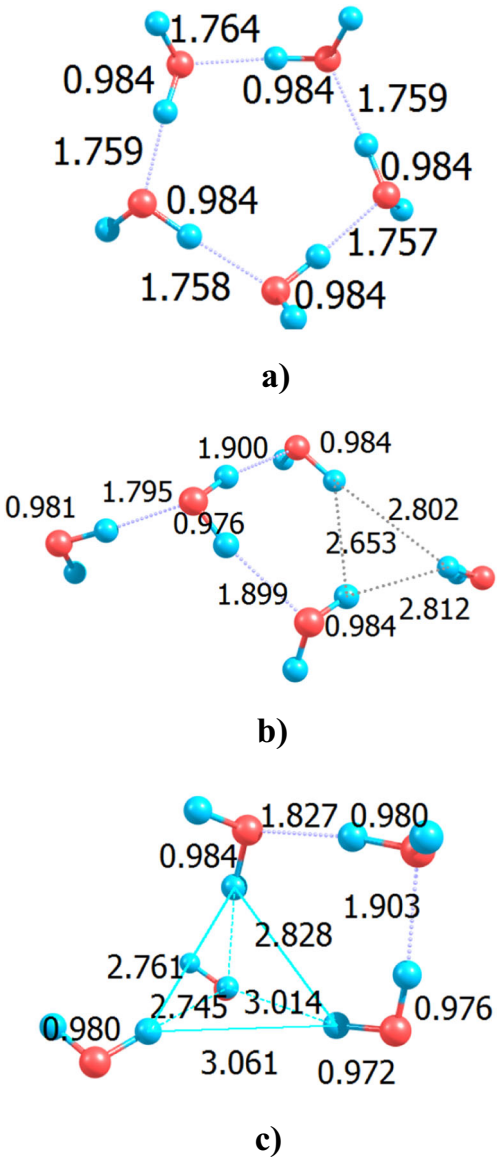

Fig. 8 Optimized geometric shapes and some bond distances (Å) in aqueous solution of **a** neutral **5n-s1**, **b** anionic **5a-s1**, and **c** anionic **5a-s2** (PCM-B3LYP/6-311++G(3df,2p)). Relative energies (ΔE, in kcal/mol) are obtained from PCM-(U)CCSD(T)/aug-cc-pVTZ + ZPE computations based on (U)B3LYP geometries

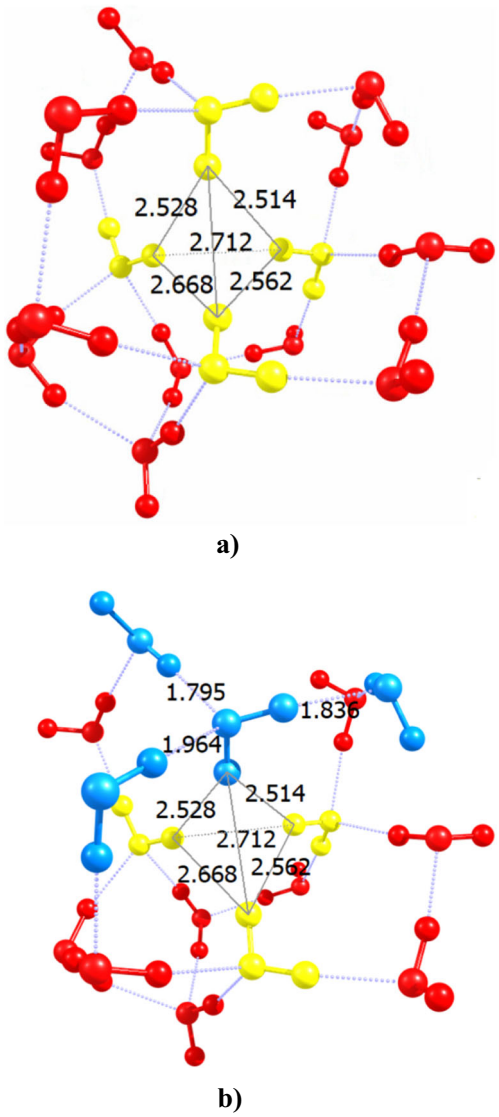

Fig. 9 Optimized geometry of $e^-(H_2O)_{16}$ in aqueous solution (PCM-UB3LYP/6-311++G(3df,2p)): **a** tetrahedral building unit is highlighted and **b** a configuration around each water molecule of the tetrahedral unit

somewhat similar to those in the gas phase **4a-g1** (Fig. 1). Attachment at possible sites around such a building block leads to a large number of isomers having comparable thermodynamic stability.

As for a representative example, Fig. 9 displays an optimized structure of $(H_2O)_{16}^{\bullet-}$ with $n = 16$. Figure 9a shows an optimized geometry of this anion in solution with highlighting of the core unit of four water molecules situated in a tetrahedral shape surrounded by twelve other water molecules. As seen in Fig. 9b, each molecule of tetrahedral core unit is connected by three molecules. Taken together, this provides us with a picture of the first solvation shell of water anion in solution.

In agreement with a recent theoretical study which also used the UB3LYP functional but with a smaller basis set [26], this result supports the view on a predominance of tetrameric unit in $(H_2O)_n^{\bullet-}$. To test further this result, we carry out geometry optimizations using the density functionals UwB97X and UwB97XD with the same 6-311++G(3df,2p) basis set, and the same geometries are found. In other words, the unit of four water molecules ($n = 4$) appears to be necessary and sufficient for the hydration of the electron through direct interactions.

Concluding remarks

In the present theoretical study, quantum chemical computations using both density functional theory (B3LYP

hybrid functional) and wavefunction (MP2 and coupled-cluster CCSD(T) theory) methods, with correlation consistent basis sets, in conjunction with a PCM approach for treating systems in aqueous solution, were carried out to have another look at the geometric structure and electron distribution of a series of small negatively charged water species $[(H_2O)_n]^{\bullet-}$. While structures in both gas phase and aqueous solution were determined by extensive geometry optimizations, the identity of the excess electron was probed using two different techniques for partitioning the total electron density (ELF and AIM). The most remarkable results emerged as follows:

i. For each size of the anionic oligomer $[(H_2O)_n]^{\bullet-}$ with n = 2, 3, and 4, two distinct structural motifs can be identified. The first is a classical water radical anion formed through hydrogen bonds that are similar to those in their neutral water counterpart. The second motif is a hydrated electron in which the electron is interacting with H atoms, each arising from one water monomer. For these small oligomers, the fact that both motifs have comparable energy content and compete for the ground state suggests their coexistence in solution.
ii. Starting from n = 5, the tetrameric anion in each motif behaves as a core unit from which larger oligomers can be built up upon successive or multiple addition of water monomers through hydrogen bonds, giving rise to a plethora of isomers having similar energy content. Four water molecules thus appear to be a minimal but sufficient number of discrete water molecules to hydrate the electron in an aqueous solution via direct electron-H atoms interactions. Such a number of water molecules is similar to the solvation process of small organic molecules in aqueous solution [48, 49]. Future theoretical studies determining spectroscopic parameters, such as the electronic absorption bands, are needed to allow both types of structures to be distinguished.

Supplementary Information The online version contains supplementary material available at https://doi.org/10.1007/s11224-021-01749-3.

Acknowledgments MTN is grateful to Prof. Andreas Savin at Universite Sorbonne Paris for valuable discussion on the ELF computation in solution.

Author contribution All authors contributed to the study conception and calculations design. TLH and LVD carried out quantum chemical computations and data collection. The first draft of the manuscript was written by MTN and edited by DM and JL, and all authors commented on the analyses and the text.

Funding TLH and MTN thank Ton Duc Thang University (Demasted) for support. JL and DM acknowledge the support of NSF-CREST (Award No. 154774).

Declarations

Consent All authors read and approved the content of the final manuscript, and all gave explicit consent to submit.

Conflict of interest The authors declare no competing interests.

Research involving human participants and/or animals Not Applicable

References

1. Simons J, Jordan KD (1987). Chem Rev 87:835
2. Neumark DM (2008). Mol Phys 106:2183
3. Hart EJ, Boag JW (1962). J Am Chem Soc 84:4090
4. Hart EJ, Anbar M (1970) The hydrated electron. Wiley Interscience, New York
5. Walker DC (1966). Quart Rev 20:77
6. Feng DF, Keven L (1980). Chem Rev 80:1
7. Rossky PJ, Schitker J (1988). J Phys Chem 92:4277
8. Barnett RN, Landman U, Scharf D, Jortner J (1989). Acc Chem Res 22:350
9. Garrett BC, Dixon DA, Camaioni DM, Chipman DM, Johnson MA, Jonah CD, Kimmel GA, Miller JH, Rescigno TN, Rossky TN (2005). Chem Rev 105:355
10. Sommerfeld T, DeFusco A, Jordan KN (2008). J Phys Chem A 112:11021
11. Ehrler OT, Neumark DN (2009). Acc Chem Res 42:769
12. Marsalek O, Uhlig F, Vandevondele J, Jungwirth P (2012). Acc Chem Res 45:23
13. Turi L, Rossky PJ (2012). Chem Rev 112:5641
14. Herbert JM (2019). Phys Chem Chem Phys 21:20538
15. Arnold ST, Eaton JG, Sarkas HW, Bowen KH (1989) In: Maier JP (ed) Ion and Cluster Ion Spectroscopy and Structure. Elsevier, Amsterdam, p 417
16. Suh SB, Lee HM, Kim J, Lee JY, Kim KS (2000). J Chem Phys 113:5273
17. Coe JV (2006). J Chem Phys 125:014315
18. Bailey CG, Kim J, Johnson MA (1996). J Phys Chem 100:16782
19. Hammer NI, Rosciolli JR, Johnson MA (2005). J Phys Chem A 109:7896
20. Jou FY, Freeman GR (1979). J Phys Chem 83:2383
21. Marbach W, Asaad AN, Krebs P (1999). J Phys Chem A 103:28
22. Hertwig A, Hippler H, Unterreiner A (1999). Phys Chem Chem Phys 1:5633
23. Herburger A, Barwa E, Oncak M, Heller J, van der Linde C, Neumark DM, Beyer MK (2019). J Am Chem Soc 141:18000
24. Han ML, Seung BS, Tarakeshwar P, Kwang SK (2005). J Chem Phys 122:044309
25. Kwang SK, Sik L, Jongseob K, Jin YL (1997). J Am Chem Soc 119:9329
26. Kumar A, Walker JA, Bartels DM, Sevilla MD (2015). J Phys Chem A 119:9148
27. Herbert JM, Jacobson LD (2011). J Phys Chem A 115:14470
28. Larsen ER, Glover JW, Schwartz JB (2010). Science 329:65
29. Turi L, Madarász A (2011). Science 331:1387
30. Jacobson DL, Herbert MJ (2011). Science 331:1387-d
31. Larsen ER, Glover JW, Schwartz JB (2011). Science 331:1387-e
32. Natori M, Watanabe T (1966). J Phys Soc Jpn 21:1573
33. Newton MD (1975). J Phys Chem 79:2795
34. Shkrob IA (2007). J Phys Chem A 111:5223
35. Sonntag CV (1987) The Chemical Basis of Radiation Biology. Taylor and Francis, London

36. Marin TW, Jonah CD, Bartels DM (2005). J Phys Chem A 109: 1843 and references therein
37. Renault JP, Vuilleumier R, Pommeret S (2008). J Phys Chem A 112:7027
38. Huyen TL, Duong LV, Nguyen MT, Lin MC (2019). Int J Chem Kinet 51:610
39. Huyen TL, Pham VT, Nguyen MT, Lin MC (2019). Chem Phys Lett 731:136604
40. Frisch MJ, Trucks GW, Schlegel HB, Scuseria GE, Robb MA, Cheeseman JR, Scalmani G, Barone V, Mennucci B, Petersson GA, Nakatsuji H, Caricato M et al. Gaussian 09 (2009) Revision E.01, Gaussian Inc., Wallingford, CT.
41. McNeill AS, Zhan C, Appel AM, Stanbury DM, Dixon DA (2020). J Phys Chem A 124:6408
42. Miertus S, Scrocco E, Tomasi T (1981). J Chem Phys 55:117
43. Silvi B, Savin A (1994). Nature 371:683
44. Bader WJF (1991). Chem Rev 91:893
45. Chipman DM (1978). J Phys Chem 82:1080
46. Hammer NI, Roscioli JR, Johnson MA, Myshakin EM, Jordan KD (2005). J Phys Chem A 109:11526
47. Hammer NI, Shin JW, Headrick JM, Diken EG, Roscioli JA, Weddle GH, Johnson MA (2004). Science 306:675
48. Nguyen MT, Raspoet G, Vanquickenborne LG, Van Duijnen PJ (1997). J Phys Chem A 101:7379
49. Nguyen MT, Matus MH, Jackson VE, Ngan VT, Rustad JR, Dixon DA (2008). J Phys Chem A 112:10386